Underactuated Source Seeking by Surge Force Tuning: Theory and Boat Experiments

Bo Wang, *Graduate Student Member, IEEE*, Sergey Nersesov, *Member, IEEE*, Hashem Ashrafiuon, *Senior Member, IEEE*, Peiman Naseradinmousavi, and Miroslav Krstić, *Fellow, IEEE*

***Abstract*— We extend source seeking algorithms, in the absence of position and velocity measurements, and with the tuning of the surge input, from velocity-actuated (unicycle) kinematic models to force-actuated generic Euler–Lagrange dynamic underactuated models. In the design and analysis, we employ a symmetric product approximation, averaging, passivity, and partial-state stability theory. The proposed control law requires only real-time measurement of the source signal at the current position of the vehicle and ensures semi-global practical uniform asymptotic stability (SPUAS) with respect to the linear motion coordinates for the closed-loop system. The performance of our source seeker with surge force tuning is illustrated with both numerical simulations and experiments of an underactuated boat.**

***Index Terms*— Averaging, extremum seeking (ES), partial-state stability, planar underactuated vehicles, symmetric product approximation.**

I. Introduction

A. Motivation

EXTREMUM seeking (ES) is a real-time model-free optimization approach that is applicable not only to static maps but also, somewhat uniquely, to dynamical systems [1]. Following the development of the ES convergence guarantees by Krstić and Wang [17] and their semi-global extension by Tan et al. [38], ES has been a flourishing research area, especially in the domain of autonomous vehicle control for finding sources of signals (electromagnetic, optical, chemical, and so on), distance-based localization, distance-based formation control, and so on. The motivation for source seeking algorithms by and large comes from the fact that global positioning system (GPS) signals are not available in unstructured environments. Besides, the cost, weight, and complexity of onboard inertial navigation systems (INSs) that do not drift over longer periods of time are prohibitive. Hence, autonomous vehicles that operate without GPS or INS benefit from source seeking capabilities.

Most real vehicles are *underactuated*, whereby underactuated it is commonly meant that the number of independent actuators of a vehicle is strictly lower than the number of its degrees of freedom (DOF), as defined by the dimension of the configuration space [4]. As a consequence of the underactuation, the control design for these vehicles is much more difficult than for fully actuated vehicles [41]. Specifically, fully actuated *mechanical system* models (comprising the kinematic and dynamic equations) can be feedback linearized into double-integrator dynamics. This is not possible for underactuated vehicles. Furthermore, unlike (first-order) nonholonomic systems, where nonintegrable constraints are imposed on system velocities (such as in the unicycle), underactuated dynamic vehicle models describe the motions constrained by nonintegrable acceleration constraints, and thus, ES algorithms developed for the first-order systems cannot be directly applied to underactuated vehicles.

B. Related Results

Given the rich variety of model types, spatial dimensions, and input tuning options for autonomous vehicles, numerous approaches for source seeking have emerged in the literature. We categorize the existing results into classical averaging-based, Lie bracket averaging-based, and symmetric product approximation-based seekers according to different types of averaging techniques.

1) Classical Averaging-Based Seekers: In [44], two source seeking schemes were proposed for vehicles modeled as single and double integrators based on periodic averaging theory. The first source seeking method for the (velocity-controlled) unicycle model was presented in [43], where the forward/surge velocity is tuned, while the angular velocity is kept at a constant nonzero value (i.e., the vehicle is perpetually turning). The second result for unicycle source seeking, as an alternative to the surge velocity tuning, was the algorithm in [5], which keeps the forward speed constant while tuning the angular velocity. The method was later modified in [9] to improve the performance, where the unicycle is allowed to slow down, as it gets close to the source by regulating the forward speed. Instead of using periodic perturbations, discrete-time stochastic ES control laws were proposed in [20] and [30] for integrator systems. A further major shift from deterministic

Manuscript received 8 May 2022; revised 4 November 2022; accepted 26 December 2022. Date of publication 12 January 2023; date of current version 22 June 2023. This work was supported in part by the U.S. Office of Naval Research under Grant N00014-19-1-2255. Recommended by Associate Editor M. Maggiore. *(Corresponding author: Hashem Ashrafiuon.)*

Bo Wang, Sergey Nersesov, and Hashem Ashrafiuon are with the Department of Mechanical Engineering, Villanova University, Villanova, PA 19085 USA (e-mail: bwang6@villanova.edu; sergey.nersesov@villanova.edu; hashem.ashrafiuon@villanova.edu).

Peiman Naseradinmousavi is with the Department of Mechanical Engineering, San Diego State University, San Diego, CA 92182 USA (e-mail: pnaseradinmousavi@sdsu.edu).

Miroslav Krstić is with the Department of Mechanical and Aerospace Engineering, University of California at San Diego, La Jolla, CA 92093 USA (e-mail: krstic@ucsd.edu).

Color versions of one or more figures in this article are available at https://doi.org/10.1109/TCST.2023.3234495.

Digital Object Identifier 10.1109/TCST.2023.3234495

1063-6536 © 2023 IEEE. Personal use is permitted, but republication/redistribution requires IEEE permission.
See https://www.ieee.org/publications/rights/index.html for more information.

Authorized licensed use limited to: University of Illinois. Downloaded on June 23,2023 at 16:27:49 UTC from IEEE Xplore. Restrictions apply.

to stochastic approaches took place with the continuous-time source seeking algorithm by Liu and Krstić, [19], which replaces sinusoidal probing with suitably filtered white noise, and where the stability analysis is conducted by novel stochastic averaging [18]. In [21], a sliding mode source seeking strategy was developed for velocity-controlled unicycles using the time derivative of the source measurements.

2) Lie Bracket Averaging-Based Seekers: A direction distinct from those employing classical averaging (periodic or stochastic)—such as in [5], [9], [19], [43], and [44]—was charted by Dürr et al. [8] who introduced a Lie bracket averaging approach. The Lie bracket averaging-based strategies were applied to source seeking of single-integrator dynamics in [8] and velocity-controlled unicycles in [7], [8], and [28], where the semi-global practical stability of the source seeking systems is guaranteed. In [34] and [37], the Lie bracket averaging-based ES approach was used in distance-based formation control for unicycles. Later, the Lie bracket averaging approach was also applied to the nth order integrator-chain dynamics in [22] and [23]. Although the methods proposed in [22], [23], and [44] can be applied to force-controlled vehicles, they all depend on certain time-varying state transformations, and the stability analysis is based on the transformed system. As a consequence, these methods require the initial velocity of the vehicle to be larger than a certain constant, which depends on the perturbation frequency. Thus, these algorithms may not guarantee convergence when the vehicle starts from rest. This is the case also with the control law in [27], where the initial angular velocity is equal to the perturbation frequency. The Lie bracket averaging approach was generalized in [11], where a broad class of control functions was presented for ES control. An adaptive ES scheme was proposed in [32], where the perturbation frequency is adaptively chosen, such that the state trajectories exactly converge to the global minimum.

3) Symmetric Product Approximation-Based Seekers: The classical averaging methods and the Lie bracket averaging approaches cannot be applied directly to a generic second-order (force-controlled) vehicle model—[44, Section 3] illustrates the need for additional compensation and analysis but applies only to a fully actuated vehicle. The *symmetric product approximation* approach, which Bullo [2] and Bullo et al. [3] introduced for vibrational control of mechanical systems, has enabled considerable further advances in force-actuated source seeking. The symmetric product approximation was first employed in source seeking with a force-controlled unicycle in [31] but assuming the availability of velocity measurements. The requirement of velocity measurements was removed by Suttner and Krstić [35]. In these two papers, the angular motion dynamics of the unicycle are assumed to be a second-order integrator. The surge force is tuned by the source seeking algorithm, while the yaw torque is set to zero or to be periodic, such that the orientation of the unicycle is a linear or periodic function of time. While these innovative works are the first to employ symmetric product approximation for source seeking of force-controlled vehicles, their model of rotational motion is simplified. In this article, we conduct a design for a suitably modeled underactuated force-controlled vehicle. In a recent alternative pursuit by Suttner [33] for fully actuated mechanical systems with strict velocity-dependent dissipation, a symmetric product approximation-based ES controller was proposed, and semi-global practical uniform asymptotic stability (SPUAS) was proven for the closed-loop system. In [36], the symmetric product approach to ES control was extended to fully actuated dissipation-free mechanical systems, where a phase-lead compensator injects damping into the system to achieve convergence. In addition, the method applies to systems on Lie groups, including 2-D and 3-D vehicle models.

C. Main Contributions

In this article, we develop a novel source seeking strategy for generic force-controlled planar underactuated vehicles. The main contributions of this work are summarized as follows.

1) We provide a theoretical foundation for ES algorithms based on symmetric product approximations. We prove that the trajectories of a class of underactuated mechanical systems can be approximated by the trajectories of corresponding *symmetric product systems*. By incorporating symmetric product approximation, averaging, passivity, and partial-state stability theory, we show that the partial-state SPUAS (P-SPUAS) of a class of underactuated mechanical systems follows from partial-state uniform global asymptotic stability (P-UGAS) of the corresponding symmetric product system.
2) We consider the dynamic model of planar vehicles, instead of considering only the kinematic model, such as in [5], [7], [28], and [43]. Furthermore, unlike the strategies presented in [22], [23], [27], [36], and [44] for fully actuated vehicles, the proposed approach applies to strictly dissipative *underactuated* vehicles, including boats/ships, planar underwater vehicles, and so on, and allows the vehicle to start from rest if desired.
3) The presented seeking scheme does not require any position or velocity measurements. It requires only real-time measurements of the source signal at the current position of the vehicle and ensures SPUAS with respect to the linear motion coordinates for the closed-loop systems. The structure of the proposed controller is exceptionally simple and easy to implement: the measured output is multiplied by a periodic signal and fed into the surge force.

D. Outline

This article is organized as follows. Preliminaries and problem formulation are given in Section II. Section III presents results on symmetric product approximations. In Section IV, we present the source seeking design and stability analysis for planar underactuated vehicles. Simulation results are shown in Section V. Experimental results are presented in Section VI. Concluding remarks are provided in Section VII. Appendixes A and B contain auxiliary results and proofs.

E. Notation

Let $\mathbb{R}^n$ denote the n-dimensional real vector space; $\mathbb{R}_{\geq 0}$ the set of all nonnegative real numbers; $|\cdot|$ the Euclidean

Authorized licensed use limited to: University of Illinois. Downloaded on June 23,2023 at 16:27:49 UTC from IEEE Xplore. Restrictions apply.

norm of vectors in $\mathbb{R}^n$. The gradient of a continuously differentiable function $f : \mathbb{R}^n \to \mathbb{R}$ is denoted by $\nabla f(x) := [(\partial f(x)/\partial x_1), \ldots, (\partial f(x)/\partial x_n)]^\top$. For real matrices $A \in \mathbb{R}^{n\times m}$, we use the matrix norm $||A|| = \sup\{|Ax| : |x| = 1\}$. For any constant $r > 0$, we use the notation $\bar{\mathcal{B}}_r^n := \{x \in \mathbb{R}^n : |x| \le r\}$ to denote a ball of radius r in $\mathbb{R}^n$. For two vector fields $f, g : \mathbb{R} \times \mathbb{R}^n \to \mathbb{R}^n$, the Lie bracket is denoted by $(\mathrm{ad}_g f)(t,x) = [g,f](t,x) := (\partial f(t,x)/\partial x)g(t,x) - (\partial g(t,x)/\partial x)f(t,x)$, and $\mathrm{ad}_g^k f := \mathrm{ad}_g^{k-1}(\mathrm{ad}_g f)$. Throughout this article, we omit the arguments of functions when they are clear from the context.

II. Problem Statement

A. Model of Planar Underactuated Vehicles

A generic planar underactuated vehicle can be modeled as a three-DOF planar rigid body with two independent control inputs. Let $\mathcal{F}_s$ denote the fixed inertial frame attached to the ground, and $\mathcal{F}_b$ the body-fixed frame attached to the center of mass of the vehicle. The position of the vehicle in $\mathcal{F}_s$ is described by (x, y), and the orientation of the vehicle is represented by θ, as shown in Fig. 1. The equations of motion of the planar underactuated vehicle are given by

$$\dot{q} = J(q)\upsilon \tag{1a}$$

$$M\dot{\upsilon} + C(\upsilon)\upsilon + D\upsilon = Gu \tag{1b}$$

where $q = [x, y, \theta]^\top \in \mathbb{R}^3$ is the configuration of the vehicle; $\upsilon = [\upsilon_x, \upsilon_y, \omega]^\top \in \mathbb{R}^3$ is the generalized velocity vector consisting of the linear velocity (υ_x, υ_y) in the body-fixed frame and the angular velocity ω; $u = [u_1, u_2]^\top \in \mathbb{R}^2$ is the control input vector; $J(q)$ is the kinematic transformation matrix given by

$$J(q) = \begin{bmatrix} \cos(\theta) & -\sin(\theta) & 0 \\ \sin(\theta) & \cos(\theta) & 0 \\ 0 & 0 & 1 \end{bmatrix}. \tag{2}$$

$M = \mathrm{diag}\{m_{11}, m_{22}, m_{33}\} > 0$ is the inertia matrix; $C(\upsilon) = -C(\upsilon)^\top$ is the Coriolis matrix. The components of vector $C(\upsilon)\upsilon$ are homogeneous polynomials in $\{\upsilon_x, \upsilon_y, \omega\}$ of degree 2 [4]. We assume that the damping matrix D is positive definite and constant, which implies that the damping force is proportional to the velocity. We also assume that the surge force and the yaw torque are the two independent control inputs, and accordingly, the input matrix G is given by

$$G = \begin{bmatrix} 1 & 0 \\ 0 & 0 \\ 0 & 1 \end{bmatrix}. \tag{3}$$

Systems (1a) and (1b) can model a wide class of planar underactuated vehicles, such as ships, planar underwater vehicles, and so on.

B. Control/Optimization Objective

Assume that the position-dependent nonlinear cost function $\rho : \mathbb{R}^2 \to \mathbb{R}_{\ge 0}$ is smooth and has a global extremum; i.e., there exists a unique $(x^\star, y^\star) \in \mathbb{R}^2$, such that

$$\nabla\rho\left(x^\star, y^\star\right) = 0 \text{ and } \nabla\rho(x,y) \neq 0 \quad \forall (x,y) \neq \left(x^\star, y^\star\right). \tag{4}$$

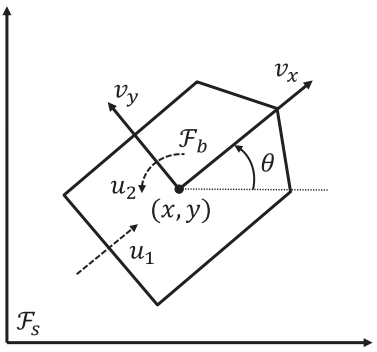

Fig. 1. Top view of the planar underactuated vehicle.

In applications, $\rho(\cdot)$ may represent the distance between the vehicle and a source, the strength of a certain (electromagnetic, optical, and so on) signal, or the concentration of chemical materials. Without loss of generality, we assume that $(x^\star, y^\star)$ is the minimum of the function ρ, and the vehicle can measure the value of $\rho(x(t), y(t))$ in real time. Note that both the extremum $(x^\star, y^\star)$ and the gradient $\nabla\rho$ are unknown. Given any constant $\varepsilon > 0$, the objective is to develop a feedback controller to steer the vehicle without position and velocity measurements, such that

$$\lim_{t\to\infty} |(x(t), y(t)) - \left(x^\star, y^\star\right)| \le \varepsilon. \tag{5}$$

C. Shifted Passivity

In the existing literature, there are generally two types of source seeking schemes for vehicle systems: 1) tuning the forward motion of the vehicle by the ES loop while keeping the angular speed constant (e.g., [8], [31], [43]) and 2) tuning the angular motion of the vehicle by the ES loop while keeping the forward velocity constant (e.g., [5], [7], [19]). In either case, the desired (linear/angular) velocity component is not zero, but instead has a steady-state value corresponding to a nonzero constant input. We formulate this property from the viewpoint of *shifted passivity* [24].

Consider systems (1a) and (1b) with the output $\eta := G^\top\upsilon$. Define the steady-state set

$$\mathcal{E} := \left\{(\upsilon, u) \in \mathbb{R}^3 \times \mathbb{R}^2 : C(\upsilon)\upsilon + D\upsilon - Gu = 0\right\}. \tag{6}$$

Fix $(\upsilon^*, u^*) \in \mathcal{E}$ and the steady-state output $\eta^* := G^\top\upsilon^*$.

Definition 1 (Shifted Passivity): Systems (1a) and (1b) are said to be *shifted passive* if the input–output mapping $(u - u^*) \mapsto (\eta - \eta^*)$ is passive; i.e., there exists a storage function $\mathcal{H} : \mathbb{R}^3 \to \mathbb{R}_{\ge 0}$, such that for all $(\upsilon, u) \in \mathbb{R}^3 \times \mathbb{R}^2$

$$\dot{\mathcal{H}} := (\nabla\mathcal{H}(\upsilon))^\top\dot{\upsilon} \le \left(u - u^*\right)^\top\left(\eta - \eta^*\right). \tag{7}$$

Proposition 1: Consider systems (1a) and (1b) with the steady-state input $u^* = [0, c]^\top$, where $c > 0$ is a constant. Then, there exists $\hat{c} > 0$, such that for all $c \in (0, \hat{c})$, systems (1a) and (1b) are shifted passive.

Proof: Fix the input $u^* = [0, c]^\top$, and the corresponding steady-state velocity and output are $\upsilon^* = [0, 0, \omega^*]^\top$ and $\eta^* = [0, \omega^*]^\top$, respectively. Let the storage function be

Authorized licensed use limited to: University of Illinois. Downloaded on June 23,2023 at 16:27:49 UTC from IEEE Xplore. Restrictions apply.

$\mathcal{H}(v) = (1/2)(v - v^*)^\top M(v - v^*)$. Then, the time derivative of $\mathcal{H}(v)$ along the trajectories of (1a) and (1b) is given by

$$\begin{aligned}\dot{\mathcal{H}} &= (v - v^*)^\top \big[G(u - u^*) - C(v)v - Dv + Gu^*\big] \\ &= (\eta - \eta^*)^\top (u - u^*) - (v - v^*)^\top \big[C(v)v + Dv - Gu^*\big] \\ &= (\eta - \eta^*)^\top (u - u^*) - (v - v^*)^\top D\big(v - v^*\big) \\ &\quad - (v - v^*)^\top \big[C(v) - C(v^*)\big]v^* \end{aligned} \tag{8}$$

where we used (1b), and added and subtracted the term Gu^* in the first identity, added and subtracted the term $(C(v) + D)v^*$ in the second identity, and used $Gu^* = C(v^*)v^* + Dv^*$ and the skew-symmetric property of $C(v)$ in the third identity. Let us denote $\mathcal{J}(v) \coloneqq C(v)v^* + Dv$. From (8) we have

$$\dot{\mathcal{H}} = (\eta - \eta^*)^\top (u - u^*) - (v - v^*)^\top \big[\mathcal{J}(v) - \mathcal{J}(v^*)\big]. \tag{9}$$

It follows from the homogeneity of $C(v)v$ that for all $v \in \mathbb{R}^3$, $||\partial[C(v)e_3]/\partial v||$ is bounded, where $e_3 = [0, 0, 1]^\top$. Thus, we can always choose ω^* small enough, such that $\partial[C(v)v^*]/\partial v + [\partial[C(v)v^*]/\partial v]^\top \leq 2D$, which implies that $(\partial\mathcal{J}(v)/\partial v) + (\partial\mathcal{J}(v)/\partial v)^\top \geq 0$ for all $v \in \mathbb{R}^3$. Therefore, the map $\mathcal{J}(\cdot)$ is monotone, and correspondingly, $(v - v^*)^\top[\mathcal{J}(v) - \mathcal{J}(v^*)] \geq 0$, which completes the proof. □

D. Partial-State Practical Stability

Consider the nonlinear interconnected system

$$\dot{x}_1 = f_1(x_1, x_2), \quad x_1(t_0) = x_{10}, \quad t \geq t_0 \tag{10}$$

$$\dot{x}_2 = f_2(x_1, x_2), \quad x_2(t_0) = x_{20} \tag{11}$$

where $f_1 : \mathbb{R}^{n_1} \times \mathbb{R}^{n_2} \to \mathbb{R}^{n_1}$ is such that, for every $x_2 \in \mathbb{R}^{n_2}$, $f_1(0, x_2) = 0$, and $f_1(x_1, x_2)$ is locally Lipschitz in x_1 uniformly in x_2; $f_2 : \mathbb{R}^{n_1} \times \mathbb{R}^{n_2} \to \mathbb{R}^{n_2}$, is such that for every $x_1 \in \mathbb{R}^{n_1}$, $f_2(x_1, x_2)$ is locally Lipschitz in x_2 uniformly in x_1. Let $x_1(\cdot) \coloneqq x_1(\cdot, x_{10}, x_{20})$ and $x_2(\cdot) \coloneqq x_2(\cdot, x_{10}, x_{20})$ denote the solution of the initial value problem (10) and (11). We define the *partial-state stability* as stability with respect to x_1 for systems (10) and (11).

Definition 2 (P-UGAS): Systems (10) and (11) are *globally asymptotically stable (GAS) with respect to x_1 uniformly in x_{20}* if the following conditions are satisfied.

1) *Partial-State Uniform Stability (P-US):* For each $\varepsilon > 0$, there exists $\delta(\varepsilon)$, such that
$$|x_{10}| \leq \delta(\varepsilon) \implies |x_1(t)| \leq \varepsilon \quad \forall t \geq 0 \ \forall x_{20} \in \mathbb{R}^{n_2}.$$
2) *Partial-State Uniform Global Boundedness (P-UGB):* For each $r > 0$, there exists $R(r)$, such that
$$|x_{10}| \leq r \implies |x_1(t)| \leq R(r) \quad \forall t \geq 0 \ \forall x_{20} \in \mathbb{R}^{n_2}.$$
3) *Partial-State Uniform Global Attractivity (P-UGA):* For each $r > 0$, for each $\sigma > 0$, there exists $T(r, \sigma)$, such that
$$|x_{10}| \leq r \implies |x_1(t)| \leq \sigma \quad \forall t \geq T(r, \sigma) \ \forall x_{20} \in \mathbb{R}^{n_2}.$$

The partial-state stability, which is also referred to as "partial stability" in the literature [10], [13], [42], is a special case of "output stability" [15], [29], [40]. By viewing x_1 as the output, the P-UGAS in Definition 2 is equivalent to the uniform global asymptotic output stability (UGAOS) [15, Definition 1] for (10) and (11).

We present Lyapunov conditions for P-UG(A)S of (10) and (11). Given a function $V(x_1, x_2)$, define $\dot{V}(x_1, x_2) = (\partial V/\partial x) f(x_1, x_2)$, where $x = [x_1^\top, x_2^\top]^\top$ and $f(x_1, x_2) = [f_1(x_1, x_2)^\top, f_2(x_1, x_2)^\top]^\top$.

Theorem 1 ([12]): Consider the interconnected system (10) and (11). If there exists a function $V : \mathbb{R}^{n_1} \times \mathbb{R}^{n_2} \to \mathbb{R}_{\geq 0}$ of class C^1, class-$\mathcal{K}_\infty$ functions α_1, α_2, such that for all $(x_1, x_2) \in \mathbb{R}^{n_1} \times \mathbb{R}^{n_2}$

$$\alpha_1(|x_1|) \leq V(x_1, x_2) \leq \alpha_2(|x_1|) \tag{12}$$

$$\dot{V}(x_1, x_2) \leq 0 \tag{13}$$

then systems (10) and (11) are US and UGB with respect to x_1 uniformly in x_{20}. Furthermore, if exists a positive definite function α_3, such that for all $(x_1, x_2) \in \mathbb{R}^{n_1} \times \mathbb{R}^{n_2}$

$$\dot{V}(x_1, x_2) \leq -\alpha_3(|x_1|) \tag{14}$$

then (10) and (11) are UGAS with respect to x_1 uniformly in x_{20}.

Next, we define *partial-state practical stability* for interconnected systems that depends on a small parameter $\varepsilon > 0$

$$\dot{x}_1 = f_1^\varepsilon(t, x_1, x_2), \quad x_1^\varepsilon(t_0) = x_{10}, \quad t \geq t_0 \tag{15}$$

$$\dot{x}_2 = f_2^\varepsilon(t, x_1, x_2). \quad x_2^\varepsilon(t_0) = x_{20}. \tag{16}$$

Let $x_1^\varepsilon(\cdot) \coloneqq x_1^\varepsilon(\cdot, t_0, x_{10}, x_{20})$ and $x_2^\varepsilon(\cdot) \coloneqq x_2^\varepsilon(\cdot, t_0, x_{10}, x_{20})$ denote the solution of the initial value problem (15) and (16).

Definition 3 (P-SPUAS): Systems (15) and (16) said to be *semi-globally practically asymptotically stable (SPAS) with respect to x_1 uniformly in (t_0, x_{20})* if for every compact set $\bar{\mathcal{B}}_r^{n_2} \subset \mathbb{R}^{n_2}$, the following conditions are satisfied.

1) For every $c_2 > 0$, there exist c_1 and $\hat{\varepsilon}(r) > 0$, such that for all $(t_0, x_{20}) \in \mathbb{R}_{\geq 0} \times \bar{\mathcal{B}}_r^{n_2}$ and for all $\varepsilon \in (0, \hat{\varepsilon})$
$$|x_{10}| \leq c_1 \implies |x_1^\varepsilon(t)| \leq c_2 \quad \forall t \geq t_0.$$
2) For every $c_1 > 0$, there exist c_2 and $\hat{\varepsilon}(r) > 0$, such that for all $(t_0, x_{20}) \in \mathbb{R}_{\geq 0} \times \bar{\mathcal{B}}_r^{n_2}$ and for all $\varepsilon \in (0, \hat{\varepsilon})$
$$|x_{10}| \leq c_1 \implies |x_1^\varepsilon(t)| \leq c_2 \quad \forall t \geq t_0.$$
3) For all $c_1 > 0$, $c_2 > 0$, there exist $T(c_1, c_2)$ and $\hat{\varepsilon}(r) > 0$, such that for all $(t_0, x_{20}) \in \mathbb{R}_{\geq 0} \times \bar{\mathcal{B}}_r^{n_2}$ and for all $\varepsilon \in (0, \hat{\varepsilon})$
$$|x_{10}| \leq c_1 \implies |x_1^\varepsilon(t)| \leq c_2 \quad \forall t \geq t_0 + T(c_1, c_2).$$

The notion of P-SPUAS is an extension of the notion of SPUAS [8], [25], [39]. It is well known that, under the assumption that trajectories of (15) and (16) converge to trajectories of (10) and (11) uniformly on compact time intervals as $\varepsilon \to 0$, if (10) and (11) are GAS, then the origin of (15) and (16) is SPUAS [25], [39]. We extend this claim to interconnected systems with partial-state stability.

Definition 4 (Partial Converging Trajectories Property): Systems (10) and (11), and (15) and (16) are said to satisfy the *partial converging trajectories property* if for every $T > 0$, for every compact set $K \subset \mathbb{R}^{n_1} \times \mathbb{R}^{n_2}$, and for

Authorized licensed use limited to: University of Illinois. Downloaded on June 23,2023 at 16:27:49 UTC from IEEE Xplore. Restrictions apply.

every $d > 0$, there exists ε^*, such that for all $t_0 \geq 0$, for all $(x_{10}, x_{20}) \in K$ and for all $\varepsilon \in (0, \varepsilon^*)$

$$|x_1^\varepsilon(t) - x_1(t)| < d \quad \forall t \in [t_0, t_0 + T]. \tag{17}$$

Proposition 2: Assume that for systems (10) and (11), the flow $[x_1(\cdot), x_2(\cdot)]$ is forward complete, and that systems (10) and (11), and (15) and (16) satisfy the partial converging trajectories property. If (10) and (11) are GAS with respect to x_1 uniformly in x_{20}, then (15) and (16) are SPAS with respect to x_1 uniformly in (t_0, x_{20}).

The proof of Proposition 2 is given in Appendix B.

III. Symmetric Product Approximations

A. Motivational Example

The classical averaging technique [43], [44] and the Lie bracket averaging approach [8] cannot be directly applied to systems (1a) and (1b). The classical averaging technique applies to systems in the form

$$\dot{\xi} = \varepsilon f(t, \xi, \varepsilon) \tag{18}$$

where $\varepsilon > 0$ is a small parameter, and f is (almost) periodic in t. However, it is not possible to find a transformation for rewriting systems (1a) and (1b) into the form (18) in general [16]. The Lie bracket averaging approach applies to input-affine systems in the form [8], [11]

$$\dot{\xi} = b_0(t, \xi) + \sum_{i=1}^{m} b_i(t, \xi)\sqrt{\omega} u_i(t, \omega t) \tag{19}$$

where $\omega \in (0, \infty)$, m is a positive integer, and the corresponding Lie bracket system is given by

$$\dot{\zeta} = b_0(t, \zeta) + \sum_{\substack{i=1 \\ j=i+1}}^{m} [b_i, b_j](t, \zeta) w_{ji}(t) \tag{20}$$

where $w_{ji}(t) = (1/T)\int_0^T u_j(t, s) \int_0^s u_i(t, \tau) \mathrm{d}\tau \mathrm{d}s$. For illustration, let us consider a damped double-integrator system

$$\begin{bmatrix} \dot{\xi}_1 \\ \dot{\xi}_2 \end{bmatrix} = \underbrace{\begin{bmatrix} \xi_2 \\ -\xi_2 \end{bmatrix}}_{b_0(\xi_2)} + \sum_{i=1}^{m} \underbrace{\begin{bmatrix} 0 \\ k_i(\xi_1) \end{bmatrix}}_{b_i(\xi_1)} u_i(t) \tag{21}$$

where $\xi_1, \xi_2, u_i \in \mathbb{R}$, $\xi = [\xi_1, \xi_2]^\top$, and the values of $k_i(\cdot)$ represent arbitrary ξ_1 (position)-dependent functions. A simple calculation shows that the Lie brackets between any two input vector fields are zero, i.e., $[b_i, b_j] \equiv 0$ for any $i, j = 1, \ldots, m$, and thus, the Lie bracket approximations cannot be applied to the double-integrator system (21), let alone systems (1a) and (1b).

Next, we will show that the symmetric product approximations can be used to solve the ES problem for (1a) and (1b). To illustrate the main idea, consider (21) again. We first change the time scale by setting $\tau = t/\varepsilon$, and let $u_i(t) = (1/\varepsilon)v_i(t/\varepsilon)$. Then, (21) becomes

$$\frac{\mathrm{d}}{\mathrm{d}\tau}\xi = \varepsilon f(\xi) + g(\tau, \xi) \tag{22}$$

where $f(\xi) = b_0(\xi_2)$, and $g(\tau, \xi) = \sum_{i=1}^m b_i(\xi_1)v_i(\tau)$. According to the variation of constants formula given in Appendix A, the corresponding *pull back system* is given by

$$\frac{\mathrm{d}}{\mathrm{d}\tau} z = \varepsilon F(\tau, z), \quad z(0) = \xi(0) \tag{23}$$

where $z = [z_1, z_2]^\top$ and

$$F(\tau, z) = f(z) + \sum_{k=1}^{\infty} \int_0^\tau \cdots \int_0^{s_{k-1}} \left(\mathrm{ad}_{g(s_k, z)} \cdots \mathrm{ad}_{g(s_1, z)} f(z)\right) \mathrm{d}s_k, \ldots, \mathrm{d}s_1.$$

By direct calculations, we have

$$\mathrm{ad}_{g(s_1, z)} f(z) = -\sum_{i=1}^{m} v_i(s_1) \begin{bmatrix} -k_i(z_1) \\ k_i(z_1) + k_i'(z_1) z_2 \end{bmatrix} \tag{24}$$

and

$$\mathrm{ad}_{g(s_2, z)} \mathrm{ad}_{g(s_1, z)} f(z) = -\sum_{i,j=1}^{m} v_i(s_1) v_j(s_2) \begin{bmatrix} 0 \\ (k_i(z_1) k_j(z_1))' \end{bmatrix}. \tag{25}$$

Note that the structural property of system (21) guarantees that the higher order terms $\mathrm{ad}_{g(s_k, z)}, \ldots, \mathrm{ad}_{g(s_1, z)} f(z) \equiv 0$ for all $k \geq 3$. Thus, the pull back vector field F can be written as follows:

$$F(\tau, z) = f(z) - \sum_{i=1}^{m} \begin{bmatrix} -k_i(z_1) \\ k_i(z_1) + k_i'(z_1) z_2 \end{bmatrix} \int_0^\tau v_i(s_1) \mathrm{d}s_1 - \sum_{i,j=1}^{m} \begin{bmatrix} 0 \\ (k_i(z_1) k_j(z_1))' \end{bmatrix} \int_0^\tau \int_0^{s_1} v_i(s_1) v_j(s_2) \mathrm{d}s_2 \mathrm{d}s_1.$$

Denote the solution of the pull back system (23) by $z(t)$. Then, it follows from the variation of constants formula in Appendix A that the solution of system (22) is given by the initial value problem:

$$\frac{\mathrm{d}}{\mathrm{d}\tau} \begin{bmatrix} \xi_1 \\ \xi_2 \end{bmatrix} = \sum_{i=1}^{m} \begin{bmatrix} 0 \\ k_i(\xi_1) \end{bmatrix} v_i(\tau), \quad \xi(0) = z(\tau). \tag{26}$$

We change the time scale back to $t = \varepsilon\tau$, and it follows from (26) that $\dot{\xi}_1 \equiv 0$, which implies that $\xi_1(t) \equiv \xi_1(0) \equiv z_1(t)$. That is, the position trajectory of the double-integrator system (21) is the z_1-trajectory of the pull back system (23).

The basic ES scheme for the double-integrator system (21) is illustrated in Fig. 2. The closed-loop system can be written as follows:

$$\begin{bmatrix} \dot{\xi}_1 \\ \dot{\xi}_2 \end{bmatrix} = \begin{bmatrix} \xi_2 \\ -\xi_2 \end{bmatrix} + \begin{bmatrix} 0 \\ h(\xi_1) \end{bmatrix} \alpha\omega \cos(\omega t) \tag{27}$$

where $h(\cdot)$ is the cost function, and $\alpha \in \mathbb{R}$ is a constant. The pull back system in time scale $\tau = t/\varepsilon = \omega t$ is given by

$$\frac{\mathrm{d}z}{\mathrm{d}\tau} = \varepsilon \left\{ f(z) - \alpha \begin{bmatrix} -h(z_1) \\ h(z_1) + h'(z_1) z_2 \end{bmatrix} \sin(\tau) - \frac{\alpha^2}{2} \begin{bmatrix} 0 \\ (h^2(z_1))' \end{bmatrix} \sin^2(\tau) \right\}.$$

Authorized licensed use limited to: University of Illinois. Downloaded on June 23,2023 at 16:27:49 UTC from IEEE Xplore. Restrictions apply.

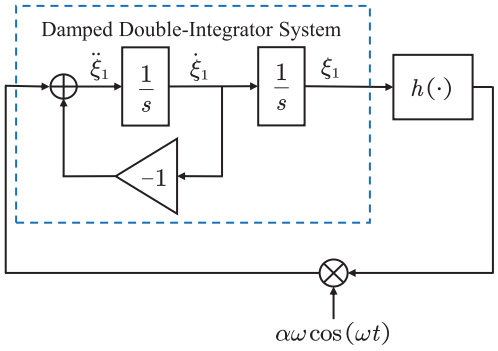

Fig. 2. ES scheme for the damped double-integrator system.

The pull back system is in the form of (18), and the averaged pull back system in time scale t is given by [16, Section 10.4]

$$\begin{bmatrix}\dot{\bar{z}}_1\\ \dot{\bar{z}}_2\end{bmatrix}=\begin{bmatrix}\bar{z}_2\\ -\bar{z}_2\end{bmatrix}-\frac{\alpha^2}{4}\begin{bmatrix}0\\ 2h(\bar{z}_1)\nabla h(\bar{z}_1)\end{bmatrix}. \tag{28}$$

Letting $V(\bar{z}_1,\bar{z}_2)=(\alpha^2/4)h^2(\bar{z}_1)+(1/2)\bar{z}_2^2$ and taking the time derivative along trajectories of (28), we have $\dot{V}=-\bar{z}_2^2\le 0$. If the cost function $h(\cdot)$ has a global minimum $h(\xi_1^\star)\ge 0$, then it follows from the Krasovskii–LaSalle principle that the global minimum is GAS. Finally, using the averaging theorem in [39] and the conclusion that $\xi_1(t)\equiv z_1(t)$, the global minimum is SPUAS for the closed-loop system (27); i.e., the position trajectory $\xi_1(t)$ converges to an $O(\varepsilon)$-neighborhood of the global minimum point $\xi_1^\star$ as $t\to\infty$. We will now generalize this idea to systems (1a) and (1b).

B. Symmetric Product Approximations

Consider systems (1a) and (1b). Let the input vector be

$$u=b_0+\frac{1}{\varepsilon}\sum_{i=1}^{m}b_i(q)w_i\left(\frac{t}{\varepsilon}\right) \tag{29}$$

where ε is a positive constant, m is a positive integer, $b_0=[b_{10},b_{20}]^\top$ is a constant vector, $b_i(q)=[b_{1i}(q),b_{2i}(q)]^\top$, and the values of $\{w_i(t)\}$ are T-periodic functions satisfying

$$\int_0^T w_i(s_1)\mathrm{d}s_1=0,\quad i=1,\dots,m \tag{30}$$

$$\int_0^T\int_0^{s_2} w_i(s_1)\mathrm{d}s_1\mathrm{d}s_2=0,\quad i=1,\dots,m. \tag{31}$$

Then, (1a) and (1b) with the input vector (29) in time scale $\tau=t/\varepsilon$ can be written as follows:

$$\frac{\mathrm{d}}{\mathrm{d}\tau}\begin{bmatrix}q\\ v\end{bmatrix}=\varepsilon\underbrace{\begin{bmatrix}J(q)v\\ -M^{-1}[C(v)v+Dv-B_0]\end{bmatrix}}_{\mathsf{f}(q,v)}+\underbrace{\begin{bmatrix}0\\ \sum_{i=1}^m B_i w_i(\tau)\end{bmatrix}}_{\mathsf{g}(\tau,q)} \tag{32}$$

where $B_0=Gb_0$, and $B_i(q)=M^{-1}Gb_i(q)$ for $i=1,\dots,m$. Denote $\mathsf{f}_2(v)=-M^{-1}[C(v)v+Dv-B_0]$. The *symmetric product* of two vector fields $X,Y:\mathbb{R}^3\to\mathbb{R}^3$ corresponding to systems (1a) and (1b) is defined as follows:

$$\langle X:Y\rangle=\frac{\partial X}{\partial q}J(q)Y+\frac{\partial Y}{\partial q}J(q)X-\left(\frac{\partial}{\partial v}\left(\frac{\partial \mathsf{f}_2}{\partial v}X\right)\right)Y. \tag{33}$$

The symmetric product $\langle\cdot:\cdot\rangle$ satisfies $\langle X:Y\rangle=\langle Y:X\rangle$.

In the next theorem, we show that systems (1a) and (1b) with input (29) can be approximated by the *symmetric product system*

$$\dot{\bar{q}}=J(\bar{q})\bar{v} \tag{34a}$$

$$M\dot{\bar{v}}+C(\bar{v})\bar{v}+D\bar{v}=B_0-M\sum_{i,j=1}^{m}\Lambda_{ij}\langle B_i:B_j\rangle(\bar{q}) \tag{34b}$$

where

$$\Lambda_{ij}=\frac{1}{2T}\int_0^T\left(\int_0^{s_1}w_i(s_2)\mathrm{d}s_2\right)\left(\int_0^{s_1}w_j(s_2)\mathrm{d}s_2\right)\mathrm{d}s_1. \tag{35}$$

Define the time-varying vector field as follows:

$$\Xi(t,q):=\sum_{i=1}^{m}\left(\int_0^t w_i(s)\mathrm{d}s\right)B_i(q). \tag{36}$$

Theorem 2: Consider systems (1a) and (1b) with input vector (29) and the symmetric product system (34a) and (34b). Assume that the initial conditions of the two systems are the same. Denote the solutions of (1a) and (1b), and (34a) and (34b) as $[q(t),v(t)]$ and $[\bar{q}(t),\bar{v}(t)]$ for $t\ge 0$, respectively. If systems (34a) and (34b) are GAS with respect to $(\bar{x},\bar{y},\bar{v}_x,\bar{v}_y)$ uniformly in $[\bar{\theta}(0),\bar{\omega}(0)]$, then systems (1a) and (1b) are SPAS with respect to (x,y,v_x,v_y) uniformly in $[\theta(0),\omega(0)]$.

Proof: By the variation of constants formula in Appendix A, the corresponding pull back system of (32) is given by

$$\frac{\mathrm{d}}{\mathrm{d}\tau}\begin{bmatrix}\hat{q}\\ \hat{v}\end{bmatrix}=\varepsilon\mathsf{F}(\tau,\hat{q},\hat{v}) \tag{37}$$

where $[\hat{q}(0),\hat{v}(0))=(q(0),v(0)]$ and

$$\mathsf{F}(\tau,q,v)=\mathsf{f}(q,v)+\sum_{k=1}^{\infty}\int_0^\tau\cdots\int_0^{s_{k-1}}\left(\mathrm{ad}_{\mathsf{g}(s_k,q)},\dots,\mathrm{ad}_{\mathsf{g}(s_1,q)}\mathsf{f}(q,v)\right)\mathrm{d}s_k,\dots,\mathrm{d}s_1.$$

By direct calculations, we have

$$\mathrm{ad}_{\mathsf{g}(s_1,z)}\mathsf{f}(q,v)=\sum_{i=1}^{m}w_i(s_1)\begin{bmatrix}J(q)B_i(q)\\ \left(\frac{\partial \mathsf{f}_2}{\partial v}\right)B_i-\left(\frac{\partial B_i}{\partial q}\right)J(q)v\end{bmatrix}$$

and

$$\mathrm{ad}_{\mathsf{g}(s_2,q)}\mathrm{ad}_{\mathsf{g}(s_1,q)}\mathsf{f}(q,v)=-\sum_{i,j=1}^{m}w_i(s_1)w_j(s_2)\begin{bmatrix}0\\ \langle B_i:B_j\rangle\end{bmatrix}.$$

Note that the symmetric product $\langle B_i:B_j\rangle$ is a vector field depending only on q. Thus, the higher order terms $\mathrm{ad}_{\mathsf{g}(s_k,q)},\dots,\mathrm{ad}_{\mathsf{g}(s_1,q)}\mathsf{f}(q,v)\equiv 0$ for all $k\ge 3$. The pull back vector field F is given by

$$\mathsf{F}=\mathsf{f}+\sum_{i=1}^{m}\begin{bmatrix}J(q)B_i(q)\\ \left(\frac{\partial \mathsf{f}_2}{\partial v}\right)B_i-\left(\frac{\partial B_i}{\partial q}\right)J(q)v\end{bmatrix}\int_0^\tau w_i(s_1)\mathrm{d}s_1-\sum_{i,j=1}^{m}\begin{bmatrix}0\\ \langle B_i:B_j\rangle\end{bmatrix}\int_0^\tau\int_0^{s_1}w_i(s_1)w_j(s_2)\mathrm{d}s_2\mathrm{d}s_1. \tag{38}$$

Authorized licensed use limited to: University of Illinois. Downloaded on June 23,2023 at 16:27:49 UTC from IEEE Xplore. Restrictions apply.

Note that system (32) is in the form of (48), and its pull back system is given by (37) and (38). Denote the solution of the pull back system (37) by $[\hat{q}(\tau), \hat{v}(\tau)]$. Then, it follows from Theorem 4 that the solution of (32) is given by the initial value problem:

$$\frac{\mathrm{d}}{\mathrm{d}\tau}\begin{bmatrix} q \\ v \end{bmatrix} = \begin{bmatrix} 0 \\ \sum_{i=1}^{m} B_i(q) w_i(\tau) \end{bmatrix}, \quad \begin{bmatrix} q(0) \\ v(0) \end{bmatrix} = \begin{bmatrix} \hat{q}(\tau) \\ \hat{v}(\tau) \end{bmatrix}. \tag{39}$$

Therefore, we have

$$q(\tau) = q(0) = \hat{q}(\tau) \tag{40}$$

$$v(\tau) = \hat{v}(\tau) + \Xi(\tau, q(\tau)). \tag{41}$$

The pull back system (37) is in the classical averaging form [16, Section 10.4]. Consider the average system

$$\frac{\mathrm{d}}{\mathrm{d}\tau}\begin{bmatrix} \bar{q} \\ \bar{v} \end{bmatrix} = \frac{\varepsilon}{T}\int_0^T \mathsf{F}(\tau, \bar{q}, \bar{v})\mathrm{d}\tau \tag{42}$$

and denote the solution by $[\bar{q}(t), \bar{v}(t)]$. It follows from (31), the symmetry of the symmetric product, and integration by parts, that the averaged system (42) in time scale $t = \varepsilon\tau$ is the symmetric product system (34a) and (34b).

According to the averaging theorem [16, Theorem 10.4], there exists $\varepsilon^* > 0$, such that for all $0 < \varepsilon < \varepsilon^*$

$$|\hat{q}(t) - \bar{q}(t)| = O(\varepsilon), \quad \text{and} \quad |\hat{v}(t) - \bar{v}(t)| = O(\varepsilon) \tag{43}$$

as $\varepsilon \to 0$ on time scale 1. We recover the partial converging trajectories property by substituting (40) and (41) into (43). Finally, it follows directly from Proposition 2 that systems (1a) and (1b) are SPAS with respect to (x, y, v_x, v_y) uniformly in $[\theta(0), \omega(0)]$, which completes the proof. □

Remark 1: In Theorem 2, instead of requiring UGAS of the symmetric product system (34a) and (34b) as in classical averaging theory [39], we only assume (34a) and (34b) to be P-UGAS with respect to $(\bar{x}, \bar{y}, \bar{v}_x, \bar{v}_y)$, while the remaining part of the state $[\bar{\theta}(t), \bar{\omega}(t)]$ does not necessarily converge to $(0, 0)$. Correspondingly, in the source seeking design in Section IV, the approximation in the linear motion $|(x, y, v_x, v_y) - (x^\star, y^\star, 0, 0)| = O(\varepsilon)$ is valid for all $t \geq 0$, while the angular motion of the vehicle can be sustained.

Remark 2: The total energy of the planar vehicle is $E = (1/2)v^\top M v$. If the vector fields $B_i(q)$ are integrable, they can be written as $B_i(q) = \nabla\varphi_i(q)$ for some scalar functions $\varphi_i(q)$, where $i = 1, \ldots, m$. It follows from [6] that if we define *symmetric product for two scalar functions* (Beltrami bracket) according to $\langle\varphi_i : \varphi_j\rangle := (\nabla\varphi_i)^\top\nabla\varphi_j$, then we have $\nabla\langle\varphi_i : \varphi_j\rangle(q) = \langle\nabla\varphi_i : \nabla\varphi_j\rangle(q) = \langle B_i : B_j\rangle(q)$. Correspondingly, the total energy of the symmetric product system (34a) and (34b) is $E_{\mathrm{av}} = (1/2)\bar{v}^\top M\bar{v} + \sum_{i,j=1}^{m}\Lambda_{ij}\langle\varphi_i : \varphi_j\rangle(\bar{q})$. The term $\sum_{i,j=1}^{m}\Lambda_{ij}\langle\varphi_i : \varphi_j\rangle(\bar{q})$, introduced by the "high-magnitude high-frequency forces," is called the *averaged potential* [3]. Thus, the control law (29) can be viewed as a "potential energy shaping" technique, where the desired potential energy function can be injected by designing appropriate input vectors $B_i(q)$. This viewpoint shows that besides the classical averaging approach in [17] and the Lie bracket averaging approach in [8], the symmetric product approximation can also be used to obtain gradient information, which will be used in the source seeking design.

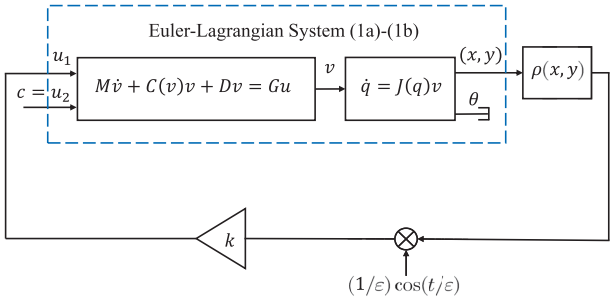

Fig. 3. Source seeking scheme for planar vehicle system (1a) and (1b).

IV. Source Seeking for Underactuated Vehicles

A. Source Seeking Scheme

We propose a source seeking scheme for the planar vehicle system (1a) and (1b), as it is depicted in Fig. 3. In the proposed scheme, the surge force of the vehicle is tuned by the ES loop, while the yaw torque keeps a certain constant value. The proposed surge force tuning-based source seeking scheme is similar to the methods in [8], [35], and [43], but will be analyzed in the symmetric product approximation framework.

The control law in Fig. 3 is given by

$$u_1 = \frac{k}{\varepsilon}\cos\left(\frac{t}{\varepsilon}\right)\rho(x, y) \tag{44}$$

$$u_2 = c \tag{45}$$

where ε, k, and c are positive parameters. The gain k is used to tune the transient performance. The small parameter ε introduces the "high-magnitude high-frequency force," which leads to the symmetric product approximation. The constant torque c maintains a sustained angular motion of the vehicle, which is necessary to establish convergence for underactuated vehicle systems.

B. Stability Analysis

Theorem 3: Consider systems (1a) and (1b) with inputs (44)–(45). Suppose that the cost function $\rho(x, y) \geq 0$ satisfies (4). Then, for any $c \in (0, \hat{c})$, $\hat{c} > 0$, and any $k > 0$, there exists $\hat{\varepsilon} > 0$, such that for the given c, k, and any $\varepsilon \in (0, \hat{\varepsilon})$, the closed-loop system is SPAS with respect to $(x - x^\star, y - y^\star, v_x, v_y)$ uniformly in $[\theta(0), \omega(0)]$.

Proof: Note that the control law (44) and (45) is in the form of (29), where $m = 1$, $b_0 = [0, c]^\top$, $b_1(q) = [k\rho(x, y), 0]^\top$, and $w_1(t) = \cos(t)$. It can be verified that conditions (30) and (31) hold for $T = 2\pi$. Thus, it follows from Theorem 2 that the closed-loop system is SPAS with respect to $(x - x^\star, y - y^\star, v_x, v_y)$ uniformly in $[\theta(0), \omega(0)]$ if the corresponding symmetric product system (34a) and (34b) is GAS with respect to $(\bar{x} - x^\star, \bar{y} - y^\star, \bar{v}_x, \bar{v}_y)$ uniformly in $[\theta(0), \omega(0)]$. Next, we show that it is indeed the case.

By direct calculations, we have $\Lambda_{11} = 1/4$, and the symmetric product is given by $\langle B_1 : B_1\rangle(\bar{q}) = 2(m_{11}^{-1}k)^2\rho(\bar{x}, \bar{y})[\rho'_x(\bar{x}, \bar{y})\cos(\bar{\theta}) + \rho'_y(\bar{x}, \bar{y})\sin(\bar{\theta}), 0, 0]^\top$, where $\rho'_x(x, y) := \partial\rho(x, y)/\partial x$, and $\rho'_y(x, y) := \partial\rho(x, y)/\partial y$. The constant torque c is selected, such

Authorized licensed use limited to: University of Illinois. Downloaded on June 23,2023 at 16:27:49 UTC from IEEE Xplore. Restrictions apply.

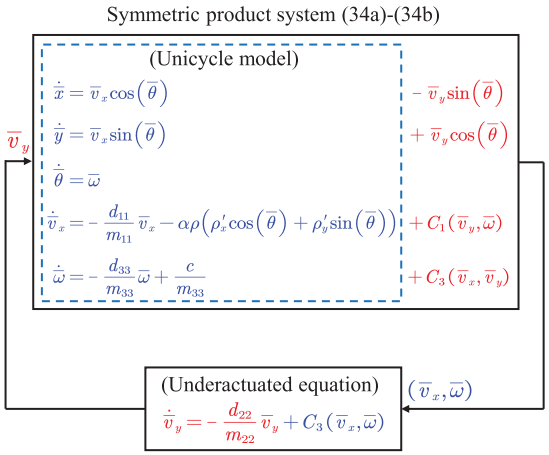

Fig. 4. Feedback interconnection of the symmetric product system (34a) and (34b).

that Proposition 1 holds, and then, systems (34a) and (34b) are shifted passive under the steady-state input $u^* = b_0$. Denote $\alpha = (m_{11}^{-1}k)^2/2$ and $C_i(\cdot)$ the ith component of the vector $-M^{-1}C(\bar{v})\bar{v}$, and note that $M^{-1}D\bar{v} = [(d_{11}/m_{11})\bar{v}_x, (d_{22}/m_{22})\bar{v}_y, (d_{33}/m_{33})\bar{\omega}]^\top$, and $M^{-1}B_0 = [0, 0, (c/m_{33})]^\top$. The symmetric product system can be viewed as a feedback interconnection of two subsystems, as shown in Fig. 4.

When the input $\bar{v}_y \equiv 0$, the nominal system of the upper subsystem is exactly the unicycle model under passive feedback. We first prove the nominal system of the upper subsystem (i.e., $\bar{v}_y \equiv 0$) is P-UGAS. Let $V_1(\bar{x}, \bar{y}, \bar{v}_x) = (1/2)\bar{v}_x^2 + (\alpha/2)\rho(\bar{x}, \bar{y})^2$, and along trajectories of the nominal system, we have $\dot{V}_1|_{\text{nominal}} = -(d_{11}/m_{11})\bar{v}_x^2 \leq 0$, which, according to Theorem 1, shows that the nominal system is US and UGB with respect to $(\bar{x} - x^\star, \bar{y} - y^\star, \bar{v}_x)$ uniformly in $[\bar{\theta}(0), \bar{\omega}(0)]$. Then, consider the auxiliary function $V_2 = \bar{v}_x \rho(\bar{x}, \bar{y})(\rho'_x \cos(\bar{\theta}) + \rho'_y \sin(\bar{\theta}))$. Evaluating the time derivative of V_2 along trajectories of the nominal system on the set $\{\bar{v}_x = 0\}$, we have $\dot{V}_2|_{\text{nominal},\bar{v}_x=0} = -\alpha\rho^2(\rho'_x \cos(\bar{\theta}) + \rho'_y \sin(\bar{\theta}))^2$, which is nonzero definite. It follows from Matrosov' theorem [13], [41] that the nominal system is UGAS with respect to $(\bar{x} - x^\star, \bar{y} - y^\star, \bar{v}_x)$ uniformly in $[\bar{\theta}(0), \bar{\omega}(0)]$.

Second, we prove that the upper subsystem is input-to-output stable (IOS) by viewing $\bar{v}_y$ as input and $(\bar{v}_x, \bar{\omega})$ as output. Because the nominal part of the upper subsystem is P-UGAS, for each $r > 0$, there exists a constant $\delta_r > 0$, such that for all initial conditions starting in the ball centering at the equilibrium with radius r, we have $\max\{|\rho'_x \cos(\bar{\theta}) + \rho'_y \sin(\bar{\theta})|, |\rho'_x \cos(\bar{\theta}) + \rho'_y \sin(\bar{\theta})|^2, |c\rho(\rho'_x \sin(\bar{\theta}) - \rho'_y \cos(\bar{\theta}))|/d_{33}, |\rho(\rho''_{xx} \cos(\bar{\theta})^2 + 2\rho''_{xy} \sin(\bar{\theta})) \cos(\bar{\theta})|\} < \delta_r$. Let $\mathcal{V}_r = \beta_r V_1 + V_2$, where $\beta_r > 0$ is a constant to be determined. It follows from Young's inequality $ab \leq a^2/(2\epsilon) + (\epsilon b^2)/2$ that $\mathcal{V}_r > 0$ and $\dot{\mathcal{V}}_r|_{\text{nominal}} \leq -\bar{v}_x^2 - (\alpha/2)\rho^2(\rho'_x \cos(\bar{\theta}) + \rho'_y \sin(\bar{\theta}))^2 + \bar{v}_x \delta_r$ by selecting $\beta_r > \max\{\delta_r^2/\alpha, 1 + 2m_{11}\delta_r/d_{11} + d_{11}/(2\alpha m_{11})\}$. Then, taking time derivative of $\mathcal{V}_r$ along trajectories of the upper subsystem, and noting that the quadratic terms $-\bar{v}_x^2 - (\alpha/2)\rho^2(\rho'_x \cos(\bar{\theta}) + \rho'_y \sin(\bar{\theta}))^2$ dominate $\dot{\mathcal{V}}_r|_{\text{upper}}$ when $|(\bar{v}_x, \rho(\rho'_x \cos(\bar{\theta}) + \rho'_y \sin(\bar{\theta})))|$ is large, we conclude that the upper subsystem is IOS with input $\bar{v}_y$ and output $(\bar{v}_x, \bar{\omega})$.

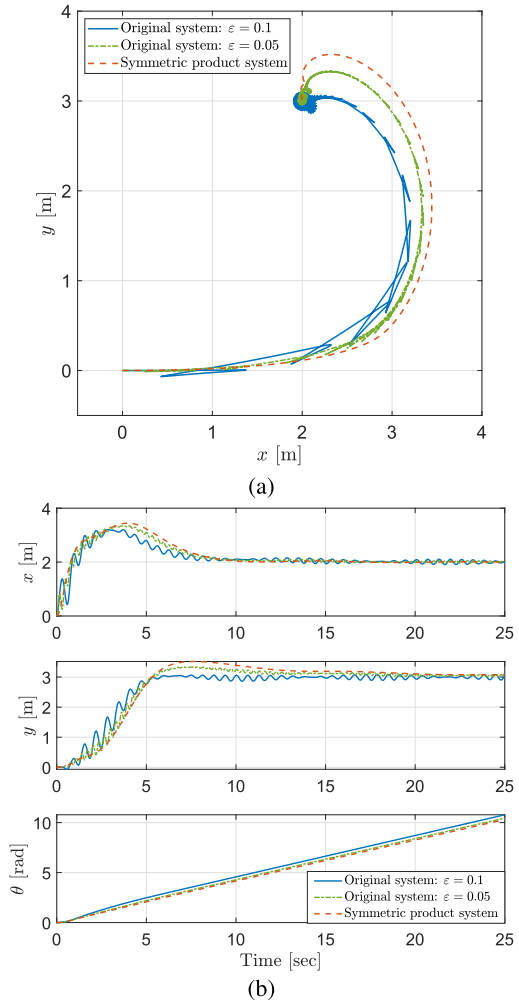

Fig. 5. Paths and configuration trajectories of the underactuated boat in source seeking ($c = 1$ and $k = 1$). (a) Paths. (b) Configuration trajectories.

Due to the fact that the lower subsystem in Fig. 4 is a stable linear system, it is also IOS by viewing $(\bar{v}_x, \bar{\omega})$ as the input and $\bar{v}_y$ as the output, and the IOS-gain can be rendered arbitrarily small by selecting c small enough. Therefore, the symmetric product system (34a) and (34b) is a feedback interconnection of two IOS subsystems, where the zero-state detectability can be easily verified. It follows from the small-gain theorem [14] that, there exists $\hat{c} > 0$, such that the symmetric product system (34a) and (34b) is GAS with respect to $(\bar{x} - x^\star, \bar{y} - y^\star, \bar{v}_x, \bar{v}_y)$ uniformly in $[\theta(0), \omega(0)]$ for all $c \in (0, \hat{c})$. Finally, we conclude that the closed-loop system is SPAS with respect to $(x - x^\star, y - y^\star, v_x, v_y)$ uniformly in $[\theta(0), \omega(0)]$ by invoking Theorem 2. □

Remark 3: Compared with the surge force tuning-based source seeking schemes in [8] and [43], the presented scheme does not require an additive periodic perturbation. The additive periodic perturbation is necessary for the Lie bracket averaging-based algorithm [8], since it is used to

Authorized licensed use limited to: University of Illinois. Downloaded on June 23,2023 at 16:27:49 UTC from IEEE Xplore. Restrictions apply.

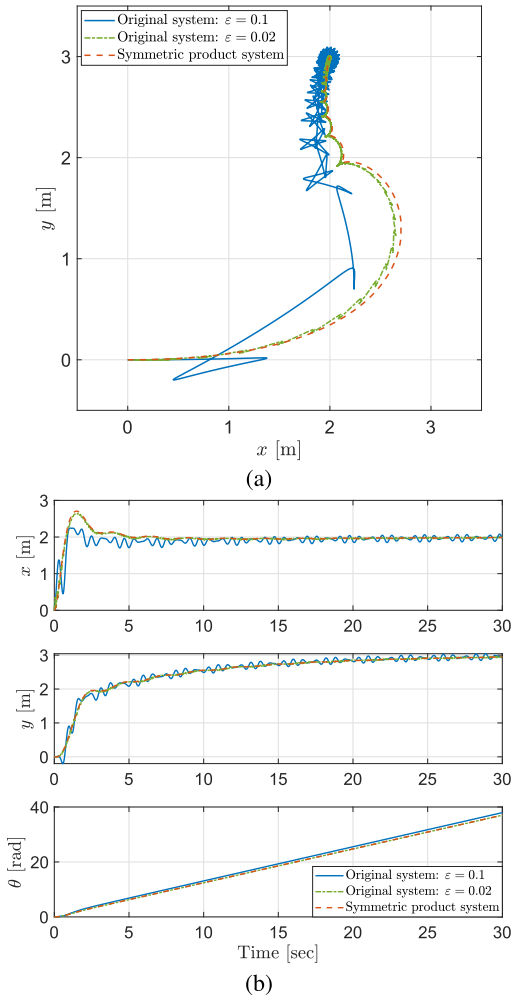

Fig. 6. Paths and configuration trajectories of the underactuated boat in source seeking ($c = 3$ and $k = 1$). (a) Paths. (b) Configuration trajectories.

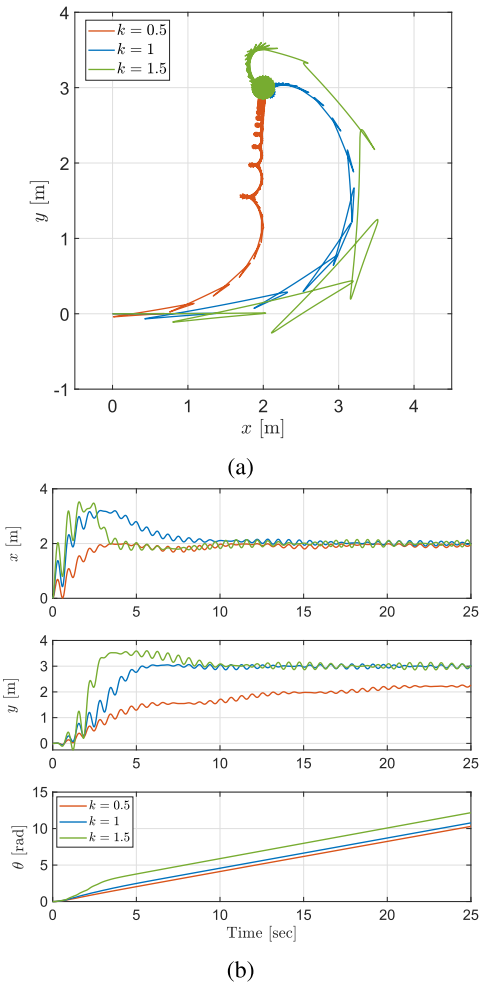

Fig. 7. Paths and configuration trajectories of the underactuated boat in source seeking ($c = 1$ and $\varepsilon = 0.1$). (a) Paths. (b) Configuration trajectories.

introduce the back-and-forth motion of a vehicle. However, as shown in Section III, only with a multiplicative periodic perturbation, the pull back system still involves an operation that is calculating Lie bracket with the vector g, i.e., $[\mathsf{g}(s_2, q), [\mathsf{g}(s_1, q), \mathsf{f}(q, v)]]$. We emphasize that the natural damping in the planar underactuated vehicle system (1a) and (1b) plays an essential role in the source seeking design and stability analysis.

V. Simulations

Consider a boat with linear hydrodynamic damping [41], where the equations are given by (1a) and (1b) with

$$C(v) = \begin{bmatrix} 0 & 0 & -m_{22}v_y \\ 0 & 0 & m_{11}v_x \\ m_{22}v_y & -m_{11}v_x & 0 \end{bmatrix}$$

and $D = \text{diag}\{d_{11}, d_{22}, d_{33}\}$, where

$$m_{11} = 1.412, \quad m_{22} = 1.982, \quad m_{33} = 0.354$$
$$d_{11} = 3.436, \quad d_{22} = 12.99, \quad d_{33} = 0.864.$$

The boat is assumed to rest at the origin initially, i.e., $(q(0), v(0)) = (0, 0)$. Assume that the cost function is $\rho(x, y) = (x-2)^2 + 0.5(y-3)^2 + 1$.

It follows from (1a) and (1b) that the constant input $(u_1^*, u_2^*) = (0, c)$ leads to the steady-state velocity $v^* = (v_x^*, v_y^*, \omega^*) = (0, 0, c/d_{33})$. Then, the constant c is chosen, such that $\partial[C(v)v^*]/\partial v + [\partial[C(v)v^*]/\partial v]^\top \leq 2D$ holds. By direct calculation, we have $4d_{11}d_{22} - (\omega^*)^2(m_{11} - m_{22})^2 \geq 0$, which implies that $c \leq 2(d_{11}d_{22})^{1/2}d_{33}/(m_{22} - m_{11}) = 20.25$. That is, with the steady-state input $u^* = [0, c]^\top$ with $c \leq 20.25$, the system is shifted passive.

In the first example, we select the control parameters in (44) and (45) to be $c = 1$ and $k = 1$. The simulation results are shown in Fig. 5 for $\varepsilon = 0.1$ and $\varepsilon = 0.05$. In the second example, we increase the constant torque to $c = 3$. The simulation results of the second example are shown in Fig. 6 for $\varepsilon = 0.1$ and $\varepsilon = 0.02$. It can be seen from both examples that the position trajectory of the underactuated boat converges to the $O(\varepsilon)$-neighborhood of the desired position $(x^\star, y^\star) = (2, 3)$. Furthermore, as $\varepsilon \to 0$, the trajectories of the boat converge to the trajectory of the symmetric product system, which represents the ideal solution. In general, a smaller ε leads to a smoother trajectory. The only limitation on the value of ε is the value of the control input (44), which increases as ε decreases. In the third example, we select the control

Authorized licensed use limited to: University of Illinois. Downloaded on June 23,2023 at 16:27:49 UTC from IEEE Xplore. Restrictions apply.

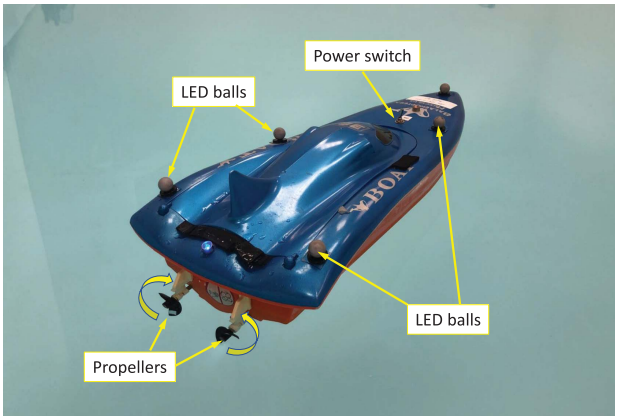

(a)

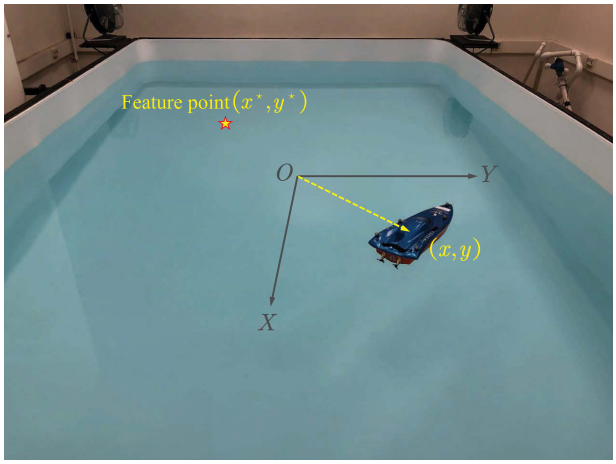

(b)

Fig. 8. Experimental boat in the water tank. (a) Boat components. (b) Boat and target positions.

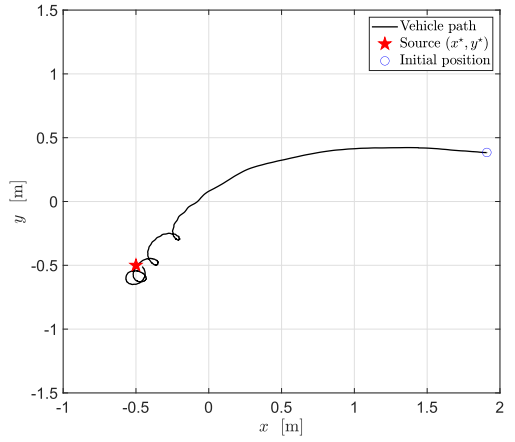

(a)

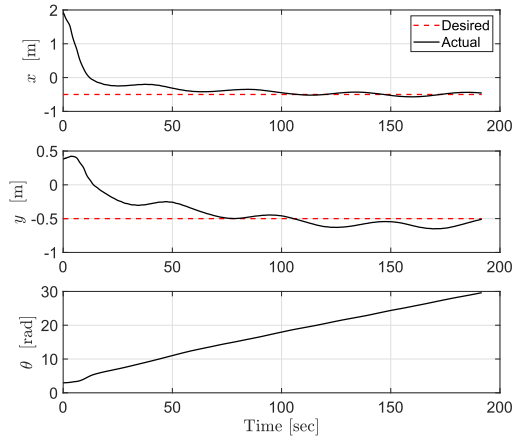

(b)

Fig. 9. Experimental path and configuration trajectories of the underactuated boat in source seeking (Case 1: $c = 2.2 \times 10^{-3}, \varepsilon = 0.5$, and $k = 0.08$). (a) Path. (b) Configuration trajectories.

parameters to be $c = 1$ and $\varepsilon = 0.1$. The simulation results are shown in Fig. 5 for $k = 0.5$, $k = 1$, and $k = 1.5$. It can be seen from Fig. 7 that increasing the gain k may improve convergence speed but results in longer paths with more dramatic winding motion.

VI. Experimental Results

To illustrate the algorithm's practicality and performance in the real world, experiments were performed with a small boat in the laboratory environment. The boat components include electronic speed control motors and propellers, a Raspberry Pi 3, a pulse width modulation (PWM) driver, and a 3000-mAh lithium polymer battery. The boat operates in a pool equipped with the Vicon motion capture system, as shown in Fig. 8. The Vicon camera system captures infrared LED balls located on the boat and provides a relative distance between the feature point (source) and the boat to the control software implemented in MATLAB/Simulink. The control signals are sent to the Raspberry Pi via a Wi-Fi router.

In the experiments, we put the feature point at the position $(x^\star, y^\star) = (-0.5, -0.5)$ m, and the boat starts from rest. In the first case, we selected the control parameters as $c = 2.2 \times 10^{-3}$, $\varepsilon = 0.5$, and $k = 0.08$. Fig. 9 shows the boat's path and pose time history and demonstrates that the boat successfully finds the source. Fig. 10 shows the boat's velocity and surge force time history. In the second case, we increased the torque and frequency by letting $c = 5.5 \times 10^{-3}$ and $\varepsilon = 0.2$ and kept $k = 0.08$. Fig. 11 shows

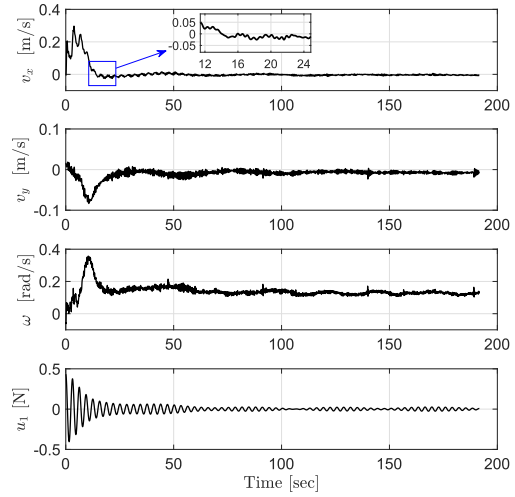

Fig. 10. Experimental velocity trajectories and the surge force of the underactuated boat in source seeking (Case 1: $c = 2.2 \times 10^{-3}, \varepsilon = 0.5$, and $k = 0.08$).

Authorized licensed use limited to: University of Illinois. Downloaded on June 23,2023 at 16:27:49 UTC from IEEE Xplore. Restrictions apply.

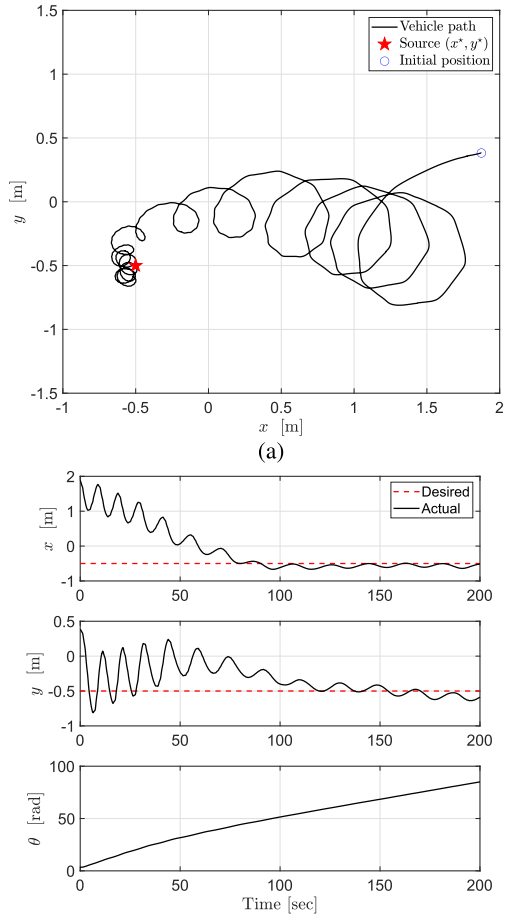

Fig. 11. Experimental path and configuration trajectories of the underactuated boat in source seeking (Case 2: $c = 5.5 \times 10^{-3}, \varepsilon = 0.2$, and $k = 0.08$). (a) Path. (b) Configuration trajectories.

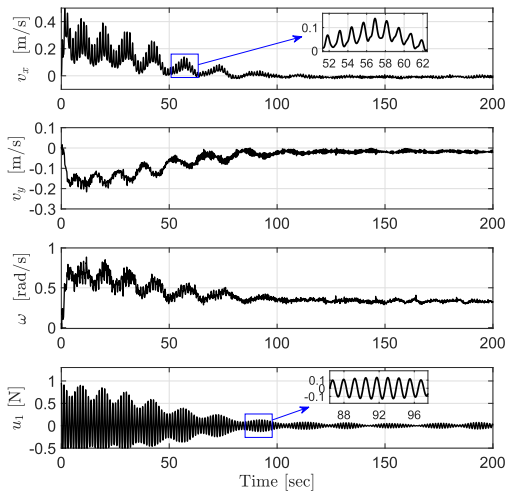

Fig. 12. Experimental velocity trajectories and the surge force of the underactuated boat in source seeking (Case 2: $c = 5.5 \times 10^{-3}, \varepsilon = 0.2$, and $k = 0.08$).

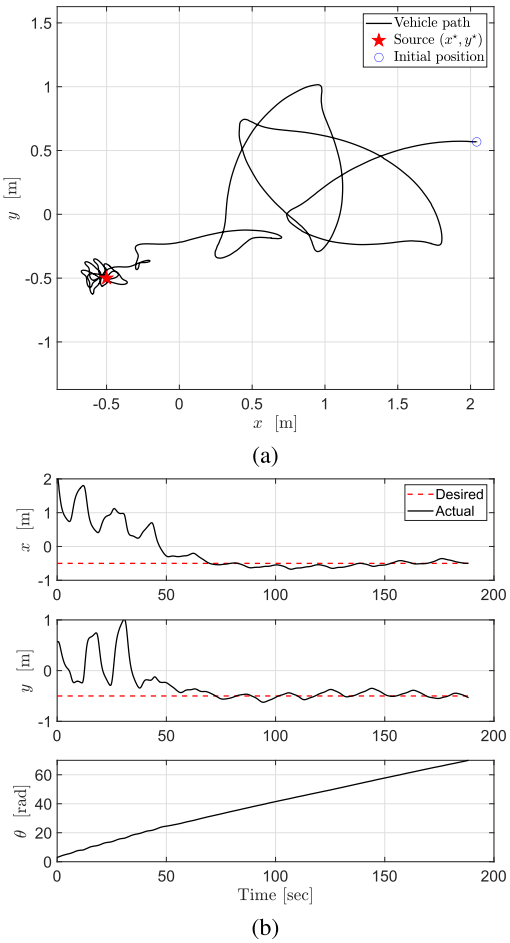

Fig. 13. Experimental path and configuration trajectories of the underactuated boat in source seeking (Case 3: $c = 5.5 \times 10^{-3}, \varepsilon = 1$, and $k = 0.33$). (a) Path. (b) Configuration trajectories.

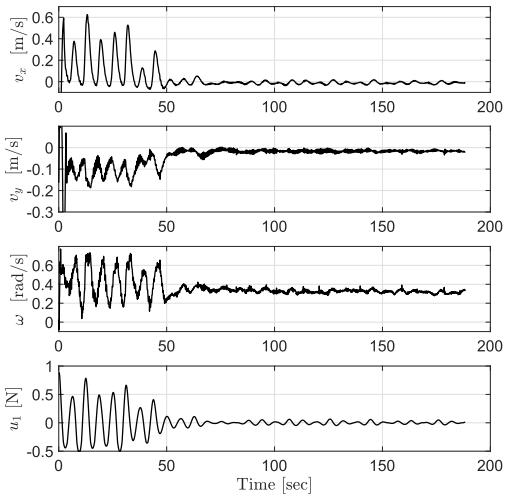

Fig. 14. Experimental velocity trajectories and the surge force of the underactuated boat in source seeking (Case 3: $c = 5.5 \times 10^{-3}, \varepsilon = 1$, and $k = 0.33$).

that the boat speeds up and goes through a higher frequency motion. As a result, the control effort is much higher to travel a larger distance without any improvement in convergence speed. Fig. 12 shows the boat's velocity and surge force time history in the second case. In the third case, we kept the higher torque value $c = 5.5 \times 10^{-3}$ but increased $\varepsilon = 1$ and $k = 0.33$. It can be seen from Fig. 13 that increasing the gain k may improve convergence speed, but on the other hand,

Authorized licensed use limited to: University of Illinois. Downloaded on June 23,2023 at 16:27:49 UTC from IEEE Xplore. Restrictions apply.

the path becomes less predictable. Fig. 14 shows the boat's velocity and surge force time history in the third case. It can be observed from Figs. 10, 12, and 14 that the boat was driven by surge force that fluctuates around zero. However, the surge velocity does not necessarily fluctuate around zero, because the backward motion of the boat has a larger damping force compared with the forward motion.

It can be seen from both the simulations and the experiments that the larger the parameter c, the faster the angular motion; the larger the parameter k, the faster the convergence speed, and the larger the parameter ε, the higher the frequency of the back-and-forth motion, but the higher the precision of the convergence. Note that the observed winding motion is typical in ES due to the use of only one signal for feedback.

VII. Conclusion

The ES design for force-controlled underactuated mechanical systems without position or velocity measurements was previously an open problem. In this work, we developed a source seeking scheme for generic force-controlled strictly dissipative planar underactuated vehicles by surge force tuning. The control design is based on symmetric product approximations, averaging, passivity, and partial-state stability theory. The controller does not require any position or velocity measurements but only real-time measurements of the source signal at the current position. The P-SPUAS is proven for the closed-loop source seeking system. Both numerical simulations and experimental results of an underactuated boat are presented to illustrate the performance of the proposed source seeker. Our future research will focus on the extension of the presented approach to multiagent source seeking [26] and source seeking for underactuated vehicles by torque tuning.

Appendix A
Variation of Constants Formula

Consider the dynamic system

$$\dot{x} = g(t, x), \quad x(0) = x_0 \tag{46}$$

where the vector field $g(t, x)$ is locally Lipschitz in x uniformly in t. The *flow map* $\Phi^g_{0,t}(\cdot)$ is a diffeomorphism, which describes the solution of (46) at time t, i.e., $x(t) = \Phi^g_{0,t}(x_0)$.

Given a diffeomorphism ϕ and a vector field f, the *pull back* of f along ϕ, denoted by $\phi^* f$, is the vector field

$$\big(\phi^* f\big)(x) := \left(\frac{\partial \phi^{-1}}{\partial x} \circ f \circ \phi\right)(x) \tag{47}$$

where $(f \circ \phi)(x) = f(\phi(x))$. The variation of constants formula [2], [4] characterizes the relationship between the flow of $f + g$ and the flows of f and g.

Theorem 4 (Variation of Constants Formula): Consider the dynamic system

$$\dot{x} = f(t, x) + g(t, x), \quad x(0) = x_0 \tag{48}$$

where the values of $f, g : \mathbb{R}_{\geq 0} \times \mathbb{R}^n \to \mathbb{R}^n$ are smooth vector fields. If $z(t)$ is the solution of the system

$$\dot{z}(t) = \Big(\big(\Phi^g_{0,t}\big)^* f\Big)(t, z), \quad z(0) = x_0 \tag{49}$$

then the solution $x(t)$ of the initial value problem

$$\dot{x} = g(t, x), \quad x(0) = z(t) \tag{50}$$

is the solution of system (48).

System (49) is called the *pull back system*. Furthermore, if f is a time-invariant vector field and g is a time-varying vector field, then the pull back of f along $\Phi^g_{0,t}$ is given by

$$\begin{aligned}&\Big(\big(\Phi^g_{0,t}\big)^* f\Big)(t, x)\\ &= f(x)\\ &\quad + \sum_{k=1}^{\infty} \int_0^t \cdots \int_0^{s_{k-1}} \big(\mathrm{ad}_{g(s_k,x)}, \ldots, \mathrm{ad}_{g(s_1,x)} f(x)\big) \mathrm{d}s_k, \ldots, \mathrm{d}s_1.\end{aligned} \tag{51}$$

Appendix B
Proof of Proposition 2

We successively prove that conditions 1–3 of Definition 3 are satisfied.

1) Take an arbitrary $c_2 > 0$, and let $b_2 \in (0, c_2)$. By the P-US property, there exists c_1, such that

$$|x_{10}| \leq c_1 \implies |x_1(t)| \leq b_2 \quad \forall t \geq t_0 \ \forall x_{20} \in \mathbb{R}^{n_2}.$$

Let $b_1 \in (0, c_1)$, and by the P-UGA property, there exists T, such that

$$|x_{10}| \leq c_1 \implies |x_1(t)| \leq b_1 \quad \forall t \geq t_0 + T \ \forall x_{20} \in \mathbb{R}^{n_2}.$$

Let $d = \min\{c_1 - b_1, c_2 - b_2\}$ and $K = \{(x_1, x_2) \in \mathbb{R}^{n_1} \times \mathbb{R}^{n_2} : |x_1| \leq c_1, |x_2| \leq r\}$, where $r > 0$ is an arbitrary number. By the partial converging trajectory property, there exists ε^*, such that for all $(x_{10}, x_{20}) \in K$ and for all $\varepsilon \in (0, \varepsilon^*)$

$$|x^\varepsilon_1(t) - x_1(t)| < d \quad \forall t \in [t_0, t_0 + T].$$

Thus, we conclude that for all $t_0 \in \mathbb{R}_{\geq 0}$, for all $(x_{10}, x_{20}) \in K$ and for all $\varepsilon \in (0, \varepsilon^*)$

$$\begin{aligned}&|x^\varepsilon_1(t)| < c_2 \quad \forall t \in [t_0, t_0 + T]\\ &|x^\varepsilon_1(t)| < c_1, \quad \text{for } t = t_0 + T.\end{aligned} \tag{52}$$

Since $|x^\varepsilon_1(t_0 + T)| < c_1$, a repeated application of (52) yields that for all $(x_{10}, x_{20}) \in K$ and for all $\varepsilon \in (0, \varepsilon^*)$, we have $|x^\varepsilon_1(t)| < c_2$, $\forall t \geq t_0$.

2) Take an arbitrary $c_1 > 0$, and let $b_1 \in (0, c_1)$. By the P-UGB and P-UGA properties, there exist b_2 and T, such that for all $t_0 \in \mathbb{R}_{\geq 0}$ and for all $x_{20} \in \mathbb{R}^{n_2}$

$$\begin{aligned}&|x_{10}| \leq c_1 \implies |x_1(t)| \leq b_2 \quad \forall t \geq t_0\\ &|x_{10}| \leq c_1 \implies |x_1(t)| \leq b_1 \quad \forall t \geq t_0 + T.\end{aligned}$$

Let $c_2 > b_2$, and by the partial converging trajectory property again, we conclude that there exists ε^*, such that for all $(x_{10}, x_{20}) \in K$ and for all $\varepsilon \in (0, \varepsilon^*)$, we have $|x^\varepsilon_1(t)| < c_2$, $\forall t \geq t_0$.

3) Take arbitrary $c_1, c_2 > 0$. By item 1) proven above, there exist c_3 and ε^*, such that for all $t_0 \in \mathbb{R}_{\geq 0}$, for all $\varepsilon \in (0, \varepsilon^*)$

$$|x_{10}| \leq c_3 \implies |x^\varepsilon_1(t)| < c_2 \quad \forall t \geq t_0 \ \forall x_{20} \in \bar{\mathcal{B}}^{n_2}_r. \tag{53}$$

Authorized licensed use limited to: University of Illinois. Downloaded on June 23,2023 at 16:27:49 UTC from IEEE Xplore. Restrictions apply.

Let $b_3 \in (0, c_3)$, and by the P-UGA property, there exists T, such that for all $x_{20} \in \mathbb{R}^{n_2}$

$$|x_{10}| \leq c_1 \implies |x_1(t)| \leq b_3 \quad \forall t \geq t_0 + T.$$

Let $d = c_3 - b_3$. Then, by the partial converging trajectory property, there exists $\varepsilon^{\#}$, such that for all $\varepsilon \in (0, \varepsilon^{\#})$ and for all $x_{20} \in \bar{\mathcal{B}}_r^{n_2}$

$$|x_{10}| \leq c_1 \implies |x_1^{\varepsilon}(t) - x_1(t)| < d \quad \forall t \in [t_0, t_0 + T]$$

which implies that for all $\varepsilon \in (0, \varepsilon^{\#})$ and for all $x_{20} \in \bar{\mathcal{B}}_r^{n_2}$

$$|x_{10}| \leq c_1 \implies |x_1^{\varepsilon}(t_0 + T)| < c_3.$$

Finally, together with (53), we conclude that for all $t_0 \in \mathbb{R}_{\geq 0}$, for all $\varepsilon \in (0, \min\{\varepsilon^*, \varepsilon^{\#}\})$, and for all $x_{20} \in \bar{\mathcal{B}}_r^{n_2}$

$$|x_{10}| \leq c_1 \implies |x_1^{\varepsilon}(t)| < c_2 \quad \forall t \geq t_0 + T$$

which completes the proof. □

REFERENCES

[1] K. B. Ariyur and M. Krstić, *Real-Time Optimization by Extremum-Seeking Control*. Hoboken, NJ, USA: Wiley, 2003.

[2] F. Bullo, "Averaging and vibrational control of mechanical systems," *SIAM J. Control Optim.*, vol. 41, no. 2, pp. 542–562, Jan. 2002.

[3] F. Bullo, N. E. Leonard, and A. D. Lewis, "Controllability and motion algorithms for underactuated Lagrangian systems on lie groups," *IEEE Trans. Autom. Control*, vol. 45, no. 8, pp. 1437–1454, Aug. 2000.

[4] F. Bullo and A. D. Lewis, *Geometric Control of Mechanical Systems: Modeling, Analysis, and Design for Simple Mechanical Control Systems*. New York, NY, USA: Springer, 2005.

[5] J. Cochran and M. Krstić, "Nonholonomic source seeking with tuning of angular velocity," *IEEE Trans. Autom. Control*, vol. 54, no. 4, pp. 717–731, Apr. 2009.

[6] P. E. Crouch, "Geometric structures in systems theory," *IEE Proc. D, Control Theory Appl.*, vol. 128, no. 5, pp. 242–252, Sep. 1981.

[7] H.-B. Dürr, M. Krstić, A. Scheinker, and C. Ebenbauer, "Extremum seeking for dynamic maps using lie brackets and singular perturbations," *Automatica*, vol. 83, pp. 91–99, Sep. 2017.

[8] H.-B. Dürr, M. S. Stanković, C. Ebenbauer, and K. H. Johansson, "Lie bracket approximation of extremum seeking systems," *Automatica*, vol. 49, no. 6, pp. 1538–1552, 2013.

[9] N. Ghods and M. Krstić, "Speed regulation in steering-based source seeking," *Automatica*, vol. 46, pp. 452–459, Feb. 2010.

[10] V. Grushkovskaya and A. Zuyev, "Partial stability concept in extremum seeking problems," *IFAC-PapersOnLine*, vol. 52, no. 16, pp. 682–687, 2019.

[11] V. Grushkovskaya, A. Zuyev, and C. Ebenbauer, "On a class of generating vector fields for the extremum seeking problem: Lie bracket approximation and stability properties," *Automatica*, vol. 94, pp. 151–160, Aug. 2018.

[12] W. M. Haddad and V. Chellaboina, *Nonlinear Dynamical Systems and Control: A Lyapunov-Based Approach*. Princeton, NJ, USA: Princeton Univ. Press, 2011.

[13] W. Hahn, *Stability of Motion*. New York, NY, USA: Springer, 1967.

[14] Z. P. Jiang, A. R. Teel, and L. Praly, "Small-gain theorem for ISS systems and applications," *Math. Control, Signals, Syst.*, vol. 7, no. 2, pp. 95–120, 1994.

[15] I. Karafyllis and A. Chaillet, "Lyapunov conditions for uniform asymptotic output stability and a relaxation of Barbălat's lemma," *Automatica*, vol. 132, Oct. 2021, Art. no. 109792.

[16] H. K. Khalil, *Nonlinear Systems*, 3rd ed. Englewood Cliffs, NJ, USA: Prentice-Hall, 2002.

[17] M. Krstić and H.-H. Wang, "Stability of extremum seeking feedback for general nonlinear dynamic systems," *Automatica*, vol. 36, no. 4, pp. 595–602, 2000.

[18] S.-J. Liu and M. Krstic, "Stochastic averaging in continuous time and its applications to extremum seeking," *IEEE Trans. Autom. Control*, vol. 55, no. 10, pp. 2235–2250, Oct. 2010.

[19] S.-J. Liu and M. Krstić, "Stochastic source seeking for nonholonomic unicycle," *Automatica*, vol. 46, no. 9, pp. 1443–1453, Sep. 2010.

[20] C. Manzie and M. Krstić, "Extremum seeking with stochastic perturbations," *IEEE Trans. Autom. Control*, vol. 54, no. 3, pp. 580–585, Mar. 2009.

[21] A. S. Matveev, H. Teimoori, and A. V. Savkin, "Navigation of a unicycle-like mobile robot for environmental extremum seeking," *Automatica*, vol. 47, no. 1, pp. 85–91, 2011.

[22] S. Michalowsky and C. Ebenbauer, "The multidimensional n-th order heavy ball method and its application to extremum seeking," in *Proc. 53rd IEEE Conf. Decis. Control*, Dec. 2014, pp. 2660–2666.

[23] S. Michalowsky and C. Ebenbauer, "Model-based extremum seeking for a class of nonlinear systems," in *Proc. Amer. Control Conf. (ACC)*, Jul. 2015, pp. 2026–2031.

[24] N. Monshizadeh, P. Monshizadeh, R. Ortega, and A. van der Schaft, "Conditions on shifted passivity of port-Hamiltonian systems," *Syst. Control Lett.*, vol. 123, pp. 55–61, Jan. 2019.

[25] L. Moreau and D. Aeyels, "Practical stability and stabilization," *IEEE Trans. Autom. Control*, vol. 45, no. 8, pp. 1554–1558, Aug. 2000.

[26] M. Sahal, T. Agustinah, and A. Jazidie, "Switching formation and topology in cooperative multi-agent source seeking using gradient estimation," in *Proc. Int. Conf. Artif. Intell. Inf. Technol. (ICAIIT)*, Mar. 2019, pp. 151–156.

[27] A. Scheinker, "Extremum seeking for force and torque actuated systems," in *Proc. 57th IEEE Conf. Decis. Control (CDC)*, Dec. 2018, pp. 7107–7111.

[28] A. Scheinker and M. Krstić, "Extremum seeking with bounded update rates," *Syst. Control Lett.*, vol. 63, pp. 25–31, Jan. 2014.

[29] E. Sontag and Y. Wang, "Lyapunov characterizations of input to output stability," *SIAM J. Control Optim.*, vol. 39, no. 1, pp. 226–249, 2000.

[30] M. S. Stanković and D. M. Stipanović, "Discrete time extremum seeking by autonomous vehicles in a stochastic environment," in *Proc. 48th IEEE Conf. Decis. Control (CDC) Held Jointly 28th Chin. Control Conf.*, Dec. 2009, pp. 4541–4546.

[31] R. Suttner, "Extremum seeking control for an acceleration controlled unicycle," *IFAC-PapersOnLine*, vol. 52, no. 16, pp. 676–681, 2019.

[32] R. Suttner, "Extremum seeking control with an adaptive dither signal," *Automatica*, vol. 101, pp. 214–222, Mar. 2019.

[33] R. Suttner, "Extremum seeking control for a class of mechanical systems," *IEEE Trans. Autom. Control*, early access, Feb. 4, 2022, doi: 10.1109/TAC.2022.3148377.

[34] R. Suttner and S. Dashkovskiy, "Exponential stability for extremum seeking control systems," *IFAC-PapersOnLine*, vol. 50, no. 1, pp. 15464–15470, Jul. 2017.

[35] R. Suttner and M. KrstiĆ, "Acceleration-actuated source seeking without position and velocity sensing," *IFAC-PapersOnLine*, vol. 53, no. 2, pp. 5348–5355, 2020.

[36] R. Suttner and M. Krstić, "Extremum seeking control for fully actuated mechanical systems on Lie groups in the absence of dissipation," 2022, *arXiv:2208.09304*.

[37] R. Suttner and Z. Sun, "Formation shape control based on distance measurements using lie bracket approximations," *SIAM J. Control Optim.*, vol. 56, no. 6, pp. 4405–4433, Jan. 2018.

[38] Y. Tan, D. Nešić, and I. Mareels, "On non-local stability properties of extremum seeking control," *Automatica*, vol. 42, pp. 889–903, Jun. 2006.

[39] A. R. Teel, J. Peuteman, and D. Aeyels, "Semi-global practical asymptotic stability and averaging," *Syst. Control Lett.*, vol. 37, no. 5, pp. 329–334, 1999.

[40] A. R. Teel and L. Praly, "A smooth Lyapunov function from a class-$\mathcal{KL}$ estimate involving two positive semidefinite functions," *ESAIM, Control, Optim. Calculus Variat.*, vol. 5, pp. 313–367, Aug. 2000.

[41] B. Wang, H. Ashrafiuon, and S. Nersesov, "Leader–follower formation stabilization and tracking control for heterogeneous planar underactuated vehicle networks," *Syst. Control Lett.*, vol. 156, Oct. 2021, Art. no. 105008.

[42] B. Wang, H. Ashrafiuon, and S. G. Nersesov, "The use of partial stability in the analysis of interconnected systems," *J. Dyn. Syst., Meas., Control*, vol. 143, no. 4, Apr. 2021.

[43] C. Zhang, D. Arnold, N. Ghods, A. Siranosian, and M. Krstić, "Source seeking with non-holonomic unicycle without position measurement and with tuning of forward velocity," *Syst. Control Lett.*, vol. 56, pp. 245–252, Mar. 2007.

[44] C. Zhang, A. Siranosian, and M. Krstić, "Extremum seeking for moderately unstable systems and for autonomous vehicle target tracking without position measurements," *Automatica*, vol. 43, pp. 1832–1839, Oct. 2007.

Authorized licensed use limited to: University of Illinois. Downloaded on June 23,2023 at 16:27:49 UTC from IEEE Xplore. Restrictions apply.

Bo Wang (Graduate Student Member, IEEE) received the M.S. degree in control theory and engineering from the University of Chinese Academy of Sciences, Beijing, China, in 2018. He is currently pursuing the Ph.D. degree with the Department of Mechanical Engineering, Villanova University, Villanova, PA, USA.

His research interests include nonlinear control theory (robust, adaptive, and passive), underactuated systems, nonholonomic systems, geometric control theory, networked control systems, extremum seeking control, and robotics.

Sergey Nersesov (Member, IEEE) received the B.S. and M.S. degrees in aerospace engineering from the Moscow Institute of Physics and Technology, Zhukovsky, Russia, in 1997 and 1999, respectively, and the M.S. degree in applied mathematics and the Ph.D. degree in aerospace engineering from the Georgia Institute of Technology, Atlanta, GA, USA, in 2003 and 2005, respectively.

He is currently an Associate Professor with the Department of Mechanical Engineering, Villanova University, Villanova, PA, USA. He has coauthored the books *Thermodynamics: A Dynamical Systems Approach* (Princeton University Press, 2005), *Impulsive and Hybrid Dynamical Systems: Stability, Dissipativity, and Control* (Princeton University Press, 2006), and *Large-Scale Dynamical Systems: A Vector Dissipative Systems Approach* (Princeton University Press, 2011). His research interests include nonlinear dynamical system theory, large-scale systems, cooperative control for multiagent systems, and hybrid and impulsive control for nonlinear systems.

Hashem Ashrafiuon (Senior Member, IEEE) received the B.S., M.S., and Ph.D. degrees from the State University of New York at Buffalo, Buffalo, NY, USA, all in mechanical engineering, in 1982, 1984, and 1988, respectively.

In 1988, he joined Villanova University, Villanova, PA, USA, as a Faculty Member, where he is currently a Professor with the Department of Mechanical Engineering. His research interests include nonlinear control of heterogeneous autonomous vehicles and underactuated systems.

Dr. Ashrafiuon is a fellow of the ASME. He is a Senior Editor of the *Journal of Vibration and Control* and has been on editorial boards of several IEEE and ASME publications.

Peiman Naseradinmousavi received the B.Sc. degree in mechanical engineering (dynamics and control) from the University of Tabriz, Tabriz, Iran, in 2002, and the Ph.D. degree in mechanical engineering (dynamics and control) from Villanova University, Villanova, PA, USA, in 2012.

He is currently an Associate Professor with the Dynamic Systems and Control Laboratory (DSCL), Department of Mechanical Engineering, San Diego State University, San Diego, CA, USA. His research interests include robotics, smart flow distribution network, nonlinear dynamics, control theory, optimization, magnetic bearings, and mathematical modeling.

Dr. Naseradinmousavi was a recipient of the John J. Gallen Memorial Alumni Award in 2021. He serves as an Associate Editor for *ASME Letters in Dynamic Systems and Control* and the *Journal of Vibration and Control (JVC)*.

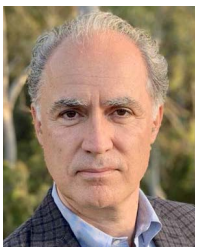

Miroslav Krstić (Fellow, IEEE) is currently a Distinguished Professor of mechanical and aerospace engineering and the Founding Director of the Cymer Center for Control Systems and Dynamics, University of California at San Diego (UCSD), La Jolla, CA, USA. He also serves as a Senior Associate Vice Chancellor for Research with UCSD. He has coauthored 16 books on adaptive, nonlinear, and stochastic control, extremum seeking, control of PDE systems including turbulent flows, and control of delay systems.

Dr. Krstić has been an elected fellow of seven scientific societies, such as IFAC, ASME, SIAM, AAAS, IET (U.K.), and AIAA (Associate Fellow), and a foreign member of the Serbian Academy of Sciences and Arts and of the Academy of Engineering of Serbia. He received the UC Santa Barbara Best Dissertation Award and the Student Best Paper Awards at CDC and ACC, as a Graduate Student. He has received the Richard E. Bellman Control Heritage Award, the SIAM Reid Prize, the ASME Oldenburger Medal, the A. V. Balakrishnan Award for Mathematics of Systems, the Nyquist Lecture Prize, the Paynter Outstanding Investigator Award, the Ragazzini Education Award, the Chestnut Textbook Prize, the Control Systems Society Distinguished Member Award, the PECASE, the NSF Career, the ONR Young Investigator Awards, the Axelby and Schuckpaper Prizes, and the first UCSD Research Award given to an Engineer. He has been awarded the Springer Visiting Professorship at UC Berkeley, the Distinguished Visiting Fellowship of the Royal Academy of Engineering, and the Invitation Fellowship of the Japan Society for the Promotion of Science. He has served as the Vice President for Technical Activities of the IEEE Control Systems Society and the Chair of the IEEE CSS Fellow Committee. He is the Alspach Endowed Chair with the University of California at San Diego (UCSD). He serves as an Editor-in-Chief for *Systems and Control Letters*. He has been serving as a Senior Editor for *Automatica* and IEEE TRANSACTIONS ON AUTOMATIC CONTROL and an Editor for two Springer book series.

Authorized licensed use limited to: University of Illinois. Downloaded on June 23,2023 at 16:27:49 UTC from IEEE Xplore. Restrictions apply.